Superfluidity Meets the Solid State: Frictionless Mass Transport through a (5,5) Carbon Nanotube

Alberto Ambrosetti,[1,*] Pier Luigi Silvestrelli,[1] and Luca Salasnich[1,2,†]
[1]*Dipartimento di Fisica e Astronomia, Università degli Studi di Padova, via Marzolo 8, 35131 Padova, Italy*
[2]*Istituto Nazionale di Fisica Nucleare, Sezione di Padova, via Marzolo 8, 35131 Padova, Italy and Istituto Nazionale di Ottica del Consiglio Nazionale delle Ricerche, Unità di Sesto Fiorentino, via Carrara 1, 50019 Sesto Fiorentino (Firenze), Italy*

(Received 20 July 2023; accepted 17 October 2023; published 13 November 2023)

Superfluidity is a well-characterized quantum phenomenon which entails frictionless motion of mesoscopic particles through a superfluid, such as ^{4}He or dilute atomic gases at very low temperatures. As shown by Landau, the incompatibility between energy and momentum conservation, which ultimately stems from the spectrum of the elementary excitations of the superfluid, forbids quantum scattering between the superfluid and the moving mesoscopic particle, below a critical speed threshold. Here, we predict that frictionless motion can also occur in the absence of a standard superfluid, i.e., when a He atom travels through a narrow (5,5) carbon nanotube (CNT). Because of the quasilinear dispersion of the plasmon and phonon modes that could interact with He, the (5,5) CNT embodies a solid-state analog of the superfluid, thereby enabling straightforward transfer of Landau's criterion of superfluidity. As a result, Landau's equations acquire broader generality and may be applicable to other nanoscale friction phenomena, whose description has been so far purely classical.

DOI: 10.1103/PhysRevLett.131.206301

Superfluidity [1–3] is a well-characterized physical phenomenon, which enables frictionless flow of a mesoscopic particle through a superfluid medium, such as ^{4}He or dilute atomic gases at very low temperatures. When the elementary excitations of the superfluid exhibit a quasilinear spectrum, twofold conservation of energy and momentum interdicts quantum-mechanical scattering, as long as the mesoscopic particle does not exceed a critical velocity threshold. Below the critical velocity, the quasi-free-particle spectrum of the mesoscopic body—which is quadratic in momentum—is incompatible with the spectrum of the superfluid, which is instead quasilinear at small momenta. Most notably, while spectral incompatibility is pivotal to superfluidity, Landau's theory [4] does not invoke particular assumptions about the nature of the medium, as long as a *free* particle can pass through. It is, thus, conceivable that seemingly disparate systems may eventually lead to analogous frictionless flow, implying nontrivial transferability of Landau's criterion of superfluidity. Known extensions of the standard mechanism contemplate, for instance, supersolidity [5,6] or even exciton condensation [7–10] in two-dimensional solid nanostructures. However, one could question the existence of *generalized-superfluid* mechanisms even in the normal state—i.e., in the absence of Bose-Einstein condensation—as long as the essential requirements are met.

To prove this idea true, in this Letter, we consider a ^{4}He atom moving through a (5,5) carbon nanotube (CNT) [11]—which can be regarded as a closed, cylindrical-shaped graphene [12] tube (see Fig. 1), characterized by a radius of 3.41 Å and longitudinal metallicity. Scattering rates will be derived from scratch, without relying on assumptions adopted in standard superfluidity (no ultracold gas is demanded). A single He atom can fit in the center of the (5,5) CNT section, and it can easily move along the longitudinal axis. The dispersion of the relevant low-energy

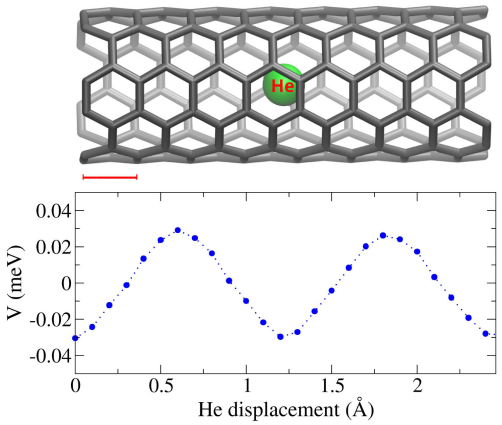

FIG. 1. Potential V_{He} computed as a function of x_{He} (He displacement) within the (5,5) CNT unit cell. C atoms are fixed in the equilibrium position, in the absence of electronic displacements. The geometry of the He atom confined in the (5,5) CNT $8 \times 1 \times 1$ supercell is illustrated for reference in the upper panel. The red segment visually indicates the longitudinal size (L) of the CNT unit cell.

quasiparticles of the CNT, i.e., plasmon and phonon excitations, bears formal analogies with the quasilinear Bogoliubov spectrum, so that the (5,5) CNT could act as an *effective superfluid medium*, providing on equal footing a viable channel for He transport. We note in passing that low-dimensional nanostructures readily attracted scientific interest in relation to superfluidity [13,14], although the presence of actual ultracold gases was so far always invoked. On the other hand, the evidence of ballistic electron transport [15,16] in CNTs adds even more appeal to these systems, also in view of their availability as C allotropes with outstanding mechanical resistance and chemical inertness.

Hereafter, we build a quantum-mechanical model, based on first-principle density functional theory (DFT) simulations, relying on semilocal [17] exchange correlation and including dispersion [18,19] corrections within Grimme's D2 [20] prescription. The approximations adopted are listed and discussed in detail in Supplemental Material [21]. The QUANTUM ESPRESSO [30] simulation package is exploited, in combination with ultrasoft pseudopotentials and an energy cutoff of 35 Ry for the plane-wave expansion of the electronic wave functions. Since we are primarily interested in the flow of a single He atom, periodic DFT simulations will minimize the interaction with periodic replicas by adoption of a long supercell (eight unit cell replicas along the CNT axis, with a total length of 19.7 Å) and setting the transversal cell size to 15 Å. The Hamiltonian describing the one-dimensional (1D) motion of a He monomer along the CNT axis (indicated as $\hat{x}$—atomic units are adopted hereafter) is

$$H_{\mathrm{He}} = -\frac{\partial^2_{x_{\mathrm{He}}}}{2m_{\mathrm{He}}} + V_{\mathrm{He}}(x_{\mathrm{He}}, \mathbf{R}_{\mathrm{ion}}, \delta\boldsymbol{\rho}_{\mathrm{el}}), \tag{1}$$

where $\mathbf{R}_{\mathrm{ion}}$ are the ionic coordinates and $\delta\boldsymbol{\rho}_{\mathrm{el}}$ the electronic charge displacements in the CNT. To investigate the problem within a perturbative framework, we initially assume that all C atoms are fixed in the equilibrium configuration and that no electronic displacement takes place. In physical terms, this corresponds to the Born-Oppenheimer (BO) approximation, in combination with the electronic ground state. Under these assumptions, the potential energy V_{He} experienced by a single He molecule traveling along the (5,5) CNT is computed by DFT. Transversal ($\hat{y} - \hat{z}$) He motion can be approximated by a 2D quantum harmonic oscillator model, whose frequency (estimated by DFT) ω_{He} is ~8 meV. As from Fig. 1, V_{He} is a sinusoidal function of x_{He} (phases can be absorbed by rigid translation): $V_{\mathrm{He}}(x_{\mathrm{He}}) \sim V \sin(2Qx_{\mathrm{He}})$, where $Q = 2\pi/L$ and L is the CNT unit cell length (i.e., 2.46 Å). The magnitude of the oscillations amounts to $V \sim 0.035$ meV (and undergoes limited change when exact exchange is included—see Ref. [21]). Dispersion interactions contribute to V with only $\sim 3 \times 10^{-4}$ meV and can, thus, be neglected. Notably, V is about 200 times smaller than ω_{He}; one accordingly expects that, for sufficiently slow He, transversal excitations can be factorized from longitudinal translations. The motion of He is, thus, effectively reduced to 1D.

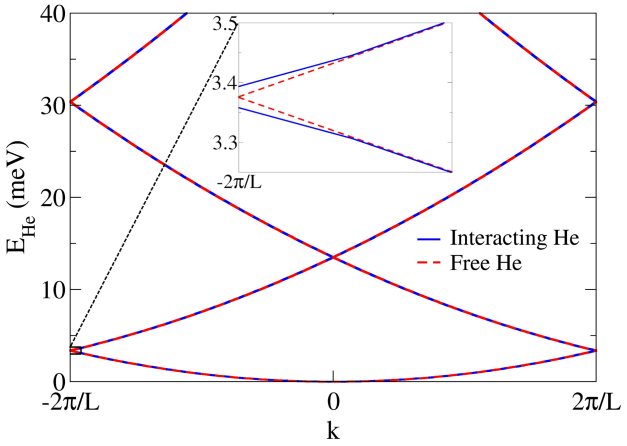

FIG. 2. Spectrum of a single He atom (longitudinal modes), subject to the potential V_{He}, as reported in Fig. 1. Since the periodicity of V_{He} corresponds to half unit cell (i.e., $L/2$), the size of the first Brillouin zone is rescaled correspondingly. Inset: detail of a band edge, where V_{He} induces small splitting.

The He spectrum relative to longitudinal motion is obtained diagonalizing the Hamiltonian Eq. (1), and it is hardly distinguishable from the free-particle dispersion $E_{\mathrm{free}}(k) = k^2/(2m_{\mathrm{He}})$, where k is the (1D) $\hat{x}$ momentum (parallel to the CNT longitudinal axis). As from Fig. 2, largest deviations are found at the Brillouin-zone edges, where small band splittings emerge due to the He-CNT coupling V_{He}. Because of the similarity between the free and interacting He spectra, one can estimate the atomic velocity as $v_{\mathrm{He}} \simeq q/m_{\mathrm{He}}$, while single plane waves provide a good approximation for He eigenstates.

Both He-phonon and He-plasmon couplings provide possible channels for the He-CNT scattering. Clearly, the spectra of the available (phononic and plasmonic) excitations play a major role in this respect, eventually determining the admitted transitions. Given the small energy scales observed so far, one can assume that the lowest-frequency modes will be most relevant. Concerning phonon excitations, the (5,5) CNT is characterized by four acoustic modes [11,31] whose frequency vanishes in the $q \to 0$ limit, according to a linear dispersion $\omega_j(q) = v_j|q|$. The index j runs over two degenerate transverse-acoustic modes (TA) with $v_{\mathrm{TA}} = 4.5 \times 10^{-3}$ a.u., a *twist* mode (TW) with $v_{\mathrm{TW}} = 6.9 \times 10^{-3}$ a.u., and longitudinal-acoustic mode (LA) with $v_{\mathrm{LA}} = 9.7 \times 10^{-3}$ a.u., according to existing [11,31] literature. A longitudinal plasmon with vanishing frequency at $q \to 0$ also exists, while transversal plasmon modes are gapped. Given the longitudinal metallicity of the (5,5) CNT, nearly 1D plasmons exhibit [32] quasilinear dispersion (up to logarithmic corrections—see Ref. [21]) in

the long-wavelength limit, and a tight-binding approach (see the full derivation in Ref. [33]) predicts typical plasmon velocities of the order of ∼1 a.u.

To address now the friction mechanism experienced by He in the CNT, we consider that a traveling He atom can scatter against the CNT, transferring part of its energy either to CNT phonon modes or to plasmons. When scattering takes place, the kinetic energy of the He atom decreases, and this is traduced into an affective friction force. To describe this process, one needs to explicitly treat both ionic ($\mathbf{R}_{\rm ion}$) and electronic ($\delta\boldsymbol{\rho}_{\rm el}$) degrees of freedom, overcoming the BO approximation. One accordingly expands the potential energy $V_{\rm He}$ to first order in both fluctuations, starting from equilibrium geometry ($\bar{\mathbf{R}}_{\rm ion}$) and zero charge displacements ($\delta\boldsymbol{\rho}_{\rm el}=0$). Ionic displacements are defined as $\delta\mathbf{R}_{\rm ion}=\mathbf{R}_{\rm ion}-\bar{\mathbf{R}}_{\rm ion}$, and the expanded potential reads

$$V_{\rm He}(x_{\rm He},\mathbf{R}_{\rm ion},\delta\boldsymbol{\rho}_{\rm el})=V_{\rm He}(x_{\rm He},\bar{\mathbf{R}}_{\rm ion},\delta\boldsymbol{\rho}_{\rm el}=0)+\sum_i\partial_{R_{i,\rm ion}}V_{\rm He}(x_{\rm He},\mathbf{R}_{\rm ion},\delta\boldsymbol{\rho}_{\rm el}=0)|_{\mathbf{R}_{\rm ion}=\bar{\mathbf{R}}_{\rm ion}}\delta R_{i,\rm ion}$$
$$+\sum_i\partial_{\delta\rho_{{\rm el},i}}V_{\rm He}(x_{\rm He},\bar{\mathbf{R}}_{\rm ion},\delta\boldsymbol{\rho}_{\rm el})|_{\delta\boldsymbol{\rho}_{\rm el}=0}\delta\rho_{{\rm el},i}+\cdots. \tag{2}$$

This expression can be physically interpreted noting that the derivatives of $V_{\rm He}$ with respect to the ionic coordinates relate to ionic forces: $\partial_{R_{i,\rm ion}}V_{\rm He}=-F_{i,\rm ion}$. Instead, the derivative with respect to the ith charge $\partial_{\rho_{{\rm el},i}}$ corresponds to an *effective potential* $\tilde{v}_i$ acting on site i. Equation (2) can, thus, be expressed in compact form as $-F_{i,\rm ion}\delta R_{i,\rm ion}+\tilde{v}_i\delta\rho_{{\rm el},i}$. Repeated indices are contracted for compactness, and the same notation will be adopted hereafter. In Eq. (2), ionic and electron-charge motions are treated as 3D, at variance with He, and they naturally account for the quasi-1D geometry of the CNT.

Both ionic and electronic-charge displacements are connected to quantum-mechanical excitation modes of the CNT, i.e., phonons and plasmons. In the case of phonons, there exists a unitary transformation that allows one to express the geometry of the jth collective vibrational modes with (1D) wave number q [i.e., $\delta\tilde{R}_j(q)$] in terms of the ionic coordinates. The transformation is $\delta\tilde{R}_j(q)=(1/\sqrt{N})S^\dagger_{j,n}e^{iql_cL}\delta R_{l_c,n,\rm ion}$, where the overall atomic index is now split into a cell index (l_c) and reduced atomic index (n), belonging to the unit cell. Here, $S_{j,n}$ is a unitary matrix that determines the geometry of the jth phonon. Calculations are formally performed in a box with finite length Λ, containing N replicas of the unit cell. The limit $\Lambda\to\infty$ is eventually taken, keeping the N/Λ unvaried. Then, by defining $\tilde{F}_j(x_{\rm He},q)=(1/\sqrt{N})S^\dagger_{j,n}e^{iql_cL}F_{l_c,n,\rm ion}(x_{\rm He})$, the term $-F_{i,\rm ion}\delta R_{i,\rm ion}$ is recast in the following form:

$$\sum_{q=0}^{N-1}\tilde{F}_j(x_{\rm He},q)\delta\tilde{R}_j(-q). \tag{3}$$

Upon quantization of the normal vibrational modes based on quantum harmonic oscillators (QHOs), Eq. (3) is expressed in terms of construction and annihilation operators ($\tilde{a}^\dagger_{j,q,\rm ion}$, $\tilde{a}_{j,q,\rm ion}$) such that

$$\delta\tilde{R}_j(q)=(\tilde{a}_{j,q,\rm ion}+\tilde{a}^\dagger_{j,q,\rm ion})/\sqrt{2m_{\rm C}\omega_j(q)}. \tag{4}$$

Here, $\omega_j(q)$ is the frequency of the jth phonon at wave number q, and $m_{\rm C}$ is the mass of a single C atom. Equation (3) provides a coupling between He and CNT phonons and can lead to scattering processes. Analogous considerations can be extended to charge displacements; hence, the He-plasmon coupling term turns out to share the same architecture as Eq. (3), although involving the specific geometry and energy spectrum of the plasmon modes (these can also be associated to QHOs, via analogous creation and annihilation operators).

We now estimate He-phonon scattering rates by Fermi's golden rule. We assume that a He atom with initial (1D) wave number $k_{{\rm He},i}$ interacts with CNT phonons via Eq. (2), ending up in the final wave number $k_{{\rm He},f}$. If the CNT initially occupies the vibrational ground state, the transition rate is

$$\Gamma^{\rm ph}_{i-f}=2\pi|\langle k_{{\rm He},f}|-F^\dagger_{i,\rm ion}|k_{{\rm He},i}\rangle\langle 1_{j,q}|\delta R_{i,\rm ion}|0_{j,q}\rangle|^2$$
$$\times\delta[E_{i,\rm He}-E_{f,\rm He}-\omega_j(q)], \tag{5}$$

where $|0_{j,q}\rangle$ and $|1_{j,q}\rangle$ are the ground state and first excited state, respectively, for the jth phonon at q. The delta function enforces energy conservation: In fact, the energy lost by He ($E_{i,\rm He}-E_{f,\rm He}$) must be converted into phonon excitation [$\omega_j(q)$]. We also note that occupation of the vibrational ground state implies a $T=0$ description. However, QHO excitation energies do not depend on the initial state.

We now make use of Eqs. (3) and (4) and consider that excitation of the jth phonon with wave number q gives $\langle 1_{j,q}|\tilde{a}^\dagger_{j,q}|0_{j,q}\rangle=1$. We also define $\Delta k_{\rm He}=k_{i,\rm He}-k_{f,\rm He}$ and note that q must be compatible with the CNT unit cell. Recalling that N unit-cell replicas are present in Λ, we facilitate normalization also assuming a finite He density;

namely, N' atoms (having the same momentum for simplicity) should be present in the adopted supercell. We also note that ionic forces can be Fourier transformed as $F_{l_c,n,\mathrm{ion}}(x_{\mathrm{He}}) = (1/2\pi)\int dq \tilde{f}_n(q) e^{iq(x_{\mathrm{He}}-l_c L)}$. After integration, Eq. (5) finally reduces to

$$\Gamma^{\mathrm{ph}}_{i-f} = 2\pi \frac{N'}{NL^2}\left|\tilde{f}_n(\Delta k_{\mathrm{He}}) S_{n,j} \frac{1}{\sqrt{2\omega_j(\Delta k_{\mathrm{He}} + mQ)m_{\mathrm{C}}}}\right|^2 \times \delta[E_{i,\mathrm{He}} - E_{f,\mathrm{He}} - \omega_j(q)]. \quad (6)$$

In the $\Lambda \to \infty$ limit, the ratios N/Λ and N'/N are kept constant in order to avoid normalization issues. When deriving the above equation, one finds that, in addition to energy conservation, *crystal momentum* is also conserved: In practice, one obtains the relation $k_{i,\mathrm{He}} = k_{f,\mathrm{He}} + q + mQ$, where m is an integer number that accounts for umklapp processes; in practice, momentum is conserved up to integer multiples of the CNT lattice momentum Q. This property stems from the discrete translational symmetry of the CNT.

As in conventional superfluids, conservation of energy and momentum is traduced into a selection rule. At low $k_{i,\mathrm{He}}$, it is possible to adopt a free-particle dispersion for He (as justified above). Hence, conservation of crystal momentum and energy is expressed as

$$\frac{k^2_{i,\mathrm{He}} - k^2_{f,\mathrm{He}}}{2m_{\mathrm{He}}} = \frac{-(q+mQ)^2 + 2k_{i,\mathrm{He}}(q+mQ)}{2m_{\mathrm{He}}} = \omega_j(q). \quad (7)$$

Equation (7) provides a generalization (due to umklapp processes) of the familiar Landau's criterion [4] of superfluidity, which gives the critical velocity below which the elastic collision is forbidden and the mesoscopic particle flows without friction. According to Eq. (7), only a limited number of $k_{i,\mathrm{He}}$ values are compatible with the excitation of the jth phonon at momentum q:

$$k_{i,\mathrm{He}} = \frac{\omega_j(q)m_{\mathrm{He}}}{q+mQ} + \frac{q+mQ}{2}. \quad (8)$$

Recalling the linear phonon dispersion in the relevant low-momentum regime $\omega_j(q) = v_j|q|$, one can examine how the solutions depend on the integer umklapp parameter m, with the aid of Fig. 3. At $m = 0$, one has conservation of the total momentum, as in conventional superfluid regimes, and the admitted interval for the initial (positive) He momenta is $k_{i,\mathrm{He}} \in [v_j m_{\mathrm{He}}, v_j m_{\mathrm{He}} + Q/2]$. Because of large phonon velocities, very high $k_{i,\mathrm{He}}$ is obtained. However, umklapp processes significantly alter this picture, as a consequence of the CNT periodicity. At $m = 1$, the allowed momentum interval becomes $k_{i,\mathrm{He}} \in [Q/2, v_j m_{\mathrm{He}}/2 + Q]$, and the lower extreme touches

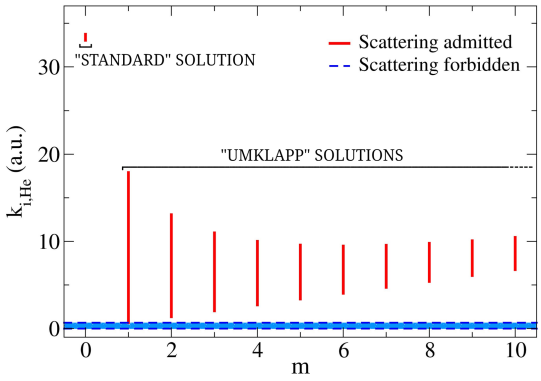

FIG. 3. Graphical representation of the solutions Eq. (8) relative to the scattering between helium and the TA phonon—analogous solutions are found for the other excitation modes that characterize the CNT. $k_{i,\mathrm{He}}$ is the wave number of He in the initial state (before the scattering takes place), and it is taken as positive. Each red segment indicates the range of $k_{i,\mathrm{He}}$ values compatible with the He-phonon scattering at a given value of the integer parameter m. When $m = 0$ (standard solution), one has exact momentum conservation ($k_{i,\mathrm{He}} - k_{f,\mathrm{He}} = q$), whereas $m \neq 0$ implies occurrence of umklapp phenomena ($k_{i,\mathrm{He}} - k_{f,\mathrm{He}} = q + mQ$). We recall that q is restricted to the Brillouin zone. In the area delimited by dashed blue lines (colored in light blue), corresponding to $k_{i,\mathrm{He}} < Q/2$, no solution is found and the scattering is forbidden.

here the minimum admitted value (q is varied between 0 and Q). As a consequence, no scattering is possible for $k_{i,\mathrm{He}} < Q/2$ (see Fig. 3); below this threshold, friction forces are expected to vanish, in close analogy to standard superfluidity. The associated speed threshold for He superflow in the (5,5) CNT is, thus, $v^*_{\mathrm{He}} = Q/(2m_{\mathrm{He}}) \sim 9.2 \times 10^{-5}$ a.u. (i.e., $\sim$200 m/s). Conversely, friction forces are restored beyond v^*_{He}. Taking $k_{i,\mathrm{He}}$ above the threshold, multiple solutions (corresponding to different m) can be found. However, one expects that large momentum transfer would be eventually associated to small scattering rates, since the Fourier-transformed ionic forces $\tilde{f}_n$ should decay at large momenta.

At variance with standard superfluidity, here the critical velocity is independent from the excitation spectrum, due to umklapp. Coming to plasmon excitations, analogous conclusions are drawn by approximating the spectrum as a linear function. Even accounting for the logarithmic corrections to linearity expected in 1D metals, no solution is possible below v^*_{He}; this unique critical velocity is sufficient to discriminate the *generalized-superfluid* regime.

By the equipartition theorem, the He kinetic energy associated to the 1D critical velocity v^*_{He} is traduced into a temperature of about 20 K; this suggests that direct injection of sufficiently slow He atoms into the CNT from a reservoir could be nontrivial. Nonetheless, major energy losses are expected when He leaves the bulk, entering the CNT edge (due to the suppression of He-He interactions

and collisions with the CNT edge); He atoms in the CNT should, thus, be slower than expected from naive considerations. In conventional superfluidity, thermal occupation of the available excitations introduces a *normal component* of the fluid, which can cause scattering and finite friction. Computation of the normal component for CNT phonons and plasmon modes (see Ref. [21]) indicates that this does not exceed ∼0.1% of the total available modes up to 300 K. The stability of the generalized-superfluidity mechanism is unparalleled and descends from the high phonon and plasmon velocities.

In summary, quantum-mechanical analysis of a He atom flowing through a subnanometer (5,5) CNT leads to a theoretical description which is formally similar (yet not identical) to Landau's superfluidity criterion. The spectrum of the CNT low-lying quasiparticle excitations (i.e., phonon and plasmon modes) is quasilinear with respect to momentum, although no Bose-Einstein condensation is assumed. This implies the existence of a critical speed $v^*_{\mathrm{He}} \simeq 200$ m/s, below which He atoms cannot scatter against the CNT, thereby encountering no friction. Remarkably, in the CNT, v^*_{He} does not depend on the excitation spectrum, as a consequence of lattice periodicity and umklapp. Indeed, we have found that $v^*_{\mathrm{He}} = Q/(2m_{\mathrm{He}})$, where $Q = 2\pi/L$ is the lattice momentum of the CNT and L its unit-cell length. While this Letter specifically addresses He flow, we expect that other rare-gas atoms (or possibly other chemical moieties) could equally move through the CNT with vanishing friction, as long as their interaction with the CNT walls is small enough to produce only weak geometrical perturbations. Analogous generalized superfluidity is expected in metallic and finite-gap CNTs with comparable radii. Experimental validation by means of nanofluidic techniques should be viable (see Ref. [21]) due to the simplicity and stability of the mechanism with respect to thermal excitations and due to the relatively high v^*_{He} value.

This Letter provides the first prediction of superfluidlike mass transport in a standard solid system and complements the ballistic electron transport already detected in CNTs. No ultracold gas is introduced here, spectral linearity is not strictly demanded at low momentum, and continuous translational invariance is not enforced. Extremely high permeabilities [34,35] (3–4 orders of magnitude larger than no-slip hydrodynamic predictions—see Ref. [21]) experimentally reported for water flow through nanoscale CNTs appear qualitatively compatible with the present findings; in fact, such measurements imply drastic suppression of friction forces (by orders of magnitude) in the limit of small CNT radii and could not be reproduced [36,37] by semiclassical models. In spite of the higher complexity of water, a generalized superfluidity mechanism may be responsible for the observed friction suppression. We add that enhanced nanofluidic flow was also confirmed in activated [38] carbon channels, and high osmotic flow was found in double-walled [39] CNTs. Extension of our quantum-mechanical theory may also interest alternative nanoscale friction [40,41] phenomena, involving, for instance, 1D and 2D heterostructures and interfaces, so that the boundary between classical and quantum-mechanical friction mechanisms should be revisited. This Letter finally opens new perspectives for nanofluidics devices, suggesting, among others, energy-efficient quantum-mechanical sieving, or nondestructive injection through cellular membranes.

A. A. and P. L. S. acknowledge funding from Cassa di Risparmio di Padova e Rovigo (CARIPARO)—grant EngvdW. A. A. acknowledges funding from the University of Padova—PARD grant. L. S. thanks Andrea Perali for useful discussions. L. S. is partially supported by the European Quantum Flagship Project "PASQuanS 2," by the European Union-NextGenerationEU within the National Center for HPC, Big Data and Quantum Computing (Project No. CN00000013, CN1 Spoke 10: "Quantum Computing"), by the BIRD Project "Ultracold atoms in curved geometries" of the University of Padova, and by "Iniziativa Specifica Quantum" of INFN. A. A. conceived this work and derived the model, carried out analytical and numerical calculations, wrote the article, and prepared figures. P. L. S. contributed to the conceptual development of the model and to *ab initio* calculations. L. S. introduced the interpretation of the phenomenon in terms of generalized superfluidity, contributed to revisions, and indicated how to perform calculations at finite T.

*Corresponding author: alberto.ambrosetti@unipd.it
†Corresponding author: luca.salasnich@unipd.it

[1] P. Kapitza, Viscosity of liquid helium below the λ-point, Nature (London) **141**, 74 (1938).
[2] J. F. Allen and A. D. Misener, Flow phenomena in liquid helium II, Nature (London) **142**, 643 (1938).
[3] A. Griffin, T. Nikuni, and E. Zaremba, *Bose-Condensed Gases at Finite Temperatures* (Cambridge University Press, Cambridge, England, 2009).
[4] L. D. Landau, E. M. Lifshitz, and L. P. Pitaevskii, *Course of Theoretical Physics*, Vol. 9: Statistical Physics, Part 2: Theory of the Condensed State (Butterworth-Heinemann, London, 1980).
[5] G. V. Chester and L. Reatto, Phonons and the properties of a Bose system, Phys. Rev. **155**, 88 (1967).
[6] L. Tanzi, E. Luiconi, F. Famá, J. Catani, A. Fioretti, C. Gabbanini, R. N. Bisset, L. Santos, and G. Modugno, Observation of a dipolar quantum gas with metastable supersolid properties, Phys. Rev. Lett. **122**, 130405 (2019).
[7] Yu. E. Lozovik and V. I. Yudson, Feasibility of superfluidity of paired spatially separated electrons and holes; a new superconductivity mechanism, JETP Lett. **22**, 274 (1975).
[8] S. De Palo, F. Rapisarda, and G. Senatore, Excitonic condensation in a symmetric electron-hole bilayer, Phys. Rev. Lett. **88**, 206401 (2002).

[9] A. A. High, J. R. Leonard, M. Remeika, L. V. Butov, M. Hanson, and C. Gossard, Condensation of excitons in a trap, Nano Lett. **12**, 2605 (2012).

[10] A. Perali, D. Neilson, and A. R. Hamilton, High-temperature superfluidity in double-bilayer graphene, Phys. Rev. Lett. **110**, 146803 (2013).

[11] M. S. Dresselhaus and P. C. Eklund, Phonons in carbon nanotubes, Adv. Phys. **49**, 705 (2000).

[12] A. Geim and K. S. Novoselov, The rise of graphene, Nat. Mater. **6**, 183 (2007).

[13] S. Moroni, F. Ancilotto, P. L. Silvestrelli, and L. Reatto, Localization versus inhomogeneous superfluidity: Submonolayer ^{4}He on fluorographene, hexagonal boron nitride, and graphene, Phys. Rev. B **103**, 174514 (2021).

[14] F. Ancilotto, M. M. Calbi, S. M. Gatica, and M. W. Cole, Bose-Einstein condensation of helium and hydrogen inside bundles of carbon nanotubes, Phys. Rev. B **70**, 165422 (2004).

[15] A. Javey, J. Guo, Q. Wang, M. Lundstrom, and H. Dai, Room carbon nanotube field-effect transistors, Nature (London) **424**, 654 (2003).

[16] P. Poncharal, C. Berger, Y. Yi, Z. L. Wang, and W. A. de Heer, Room temperature ballistic conduction in carbon nanotubes, J. Phys. Chem. B **106**, 12104 (2002).

[17] J. P. Perdew, K. Burke, and M. Ernzerhof, Generalized gradient approximation made simple, Phys. Rev. Lett. **77**, 3865 (1996).

[18] A. Ambrosetti, N. Ferri, R. A. DiStasio Jr., and A. Tkatchenko, Wavelike charge density fluctuations and van der Waals interactions at the nanoscale, Science **351**, 6278 (2016).

[19] M. Ricci, P. L. Silvestrelli, and A. Ambrosetti, Exact sum-rule approach to polarizability and asymptotic van der Waals functionals—derivation of exact single-particle benchmarks, J. Phys. Chem. Lett. **13**, 8298 (2022).

[20] S. Grimme, Semiempirical GGA-type density functional constructed with a long-range dispersion correction, Comput. Chem. **27**, 1787 (2006).

[21] See Supplemental Material at http://link.aps.org/supplemental/10.1103/PhysRevLett.131.206301, which includes Refs. [22–29], for details on the approximations introduced, experimental implications, and finite-temperature effects.

[22] J. P. Perdew, A. Ruzsinszky, G. I. Csonka, O. A. Vydrov, G. E. Scuseria, L. A. Constantin, X. Zhou, and K. Burke, Restoring the density-gradient expansion for exchange in solids and surfaces, Phys. Rev. Lett. **100**, 136406 (2008).

[23] C. Adamo and V. Barone, Toward reliable density functional methods without adjustable parameters: The PBE0 model, J. Chem. Phys. **110**, 6158 (1999).

[24] P. B. Calio, G. M. Hocky, and G. A. Voth, Minimal experimental bias on the hydrogen bond greatly improves *Ab Initio* molecular dynamics simulations of water, J. Chem. Theory Comput. **16**, 5675 (2020).

[25] A. Ambrosetti, S. Subashchandrabose, B. Liu, and P. L. Silvestrelli, Tunable van der Waals interactions in low-dimensional nanostructures, J. Chem. Phys. **154**, 224105 (2021).

[26] Y. Murakami, Y. Miyauchi, S. Chiashi, and S. Maruyama, Direct synthesis of high-quality single-walled carbon nanotubes on silicon and quartz substrates, Chem. Phys. Lett. **377**, 49 (2003).

[27] H. Dai, Carbon nanotubes: Synthesis, integration, and properties, Acc. Chem. Res. **35**, 1035 (2002).

[28] R. B. Bird, W. E. Stewart, and E. N. Lightfoot, *Transport Phenomena*, 2nd ed. (Wiley, New York, 2005).

[29] A. Ambrosetti, G. Palermo, and P. L. Silvestrelli, Quantum-mechanically enhanced water flow in subnanometer carbon nanotubes, J. Phys. Chem. C **126**, 20174 (2022).

[30] P. Giannozzi *et al.*, QUANTUM ESPRESSO: A modular and open-source software project for quantum simulations of materials, J. Phys. Condens. Matter **21**, 39 (2009).

[31] H. W. Zhang, Z. Yao, J. B. Wang, and W. X. Zhong, Phonon dispersion analysis of carbon nanotubes based on inter-belt model and symplectic solution method, Int. J. Solids Struct. **44**, 6428 (2007).

[32] J. F. Dobson, A. White, and A. Rubio, Asymptotics of the dispersion interaction: Analytic benchmarks for van der Waals energy functionals, Phys. Rev. Lett. **96**, 073201 (2006).

[33] J. F. Dobson and A. Ambrosetti, MBD + C: How to include metallic character (Type C non-additivity) into atom-based dispersion energy scheme, J. Chem. Theory Comput. **19**, 6434 (2023).

[34] M. Majumder, N. Chopra, R. Andrews, and B. J. Hinds, Nanoscale hydrodynamics: enhanced flow in carbon nanotubes, Nature (London) **438**, 44 (2005).

[35] J. K. Holt, H. G. Park, Y. Wang, M. Stadermann, A. B. Artyukhin, C. P. Grigoropoulos, A. Noy, and O. Bakajin, Fast mass transport through sub-2-nanometer carbon nanotubes, Science **312**, 1034 (2006).

[36] D. Mattia and F. Calabró, Explaining high flow rate of water in carbon nanotubes via solid-liquid molecular interactions, Microfluid. Nanofluid. **13**, 125 (2012).

[37] S. K. Kannam, B. D. Todd, J. S. Hansen, and P. J. Daivis, How fast does water flow in carbon nanotubes?, J. Chem. Phys. **138**, 094701 (2013).

[38] T. Emmerich, K. S. Vasu, A. Nigués, A. Keerthi, B. Radha, A. Siria, and L. Bocquet, Enhanced nanofluidic transport in activated carbon nanoconduits, Nat. Mater. **21**, 696 (2022).

[39] G. Cui, Z. Xu, H. Li, S. Zhang, L. Xu, A. Siria, and M. Ma, Enhanced osmotic transport in individual double-walled carbon nanotube, Nat. Commun. **14**, 2295 (2023).

[40] A. Ambrosetti, F. Ancilotto, and P. L. Silvestrelli, van der Waals-corrected *ab initio* study of water ice–graphite interaction, J. Phys. Chem. C **117**, 321 (2013).

[41] M. Dienwiebel, G. S. Verhoeven, N. Pradeep, J. W. M. Frenken, J. A. Heimberg, and H. W. Zandbergen, Superlubricity of graphite, Phys. Rev. Lett. **92**, 126101 (2004).